SZENT ISTVÁN UNIVERSITY

FAILURE CHARACTERISTICS OF BIOLOGICAL MATERIALS

Thesis of the doctoral (PhD) dissertation

Csaba Farkas

Gödöllő - Hungary
2020

Doctoral school denomination: Doctoral School of Mechanical Engineering

Science: Agricultural Engineering

Head of school: Prof. Dr. István Farkas, DSc
Faculty of Mechanical Engineering
Szent István University, Gödöllő - Hungary

Supervisor: Prof. Dr. László Fenyvesi, PhD
Institute of Machinery and Informatics
Faculty of Mechanical Engineering
Szent István University, Gödöllő - Hungary

Co-Supervisor: Dr. Károly Petróczki, PhD
Institute of Process Engineering
Faculty of Mechanical Engineering
Szent István University, Gödöllő - Hungary

. . . .
Affirmation of head of school Affirmation of supervisor

CONTENTS

LIST OF SYMBOLS

E_{c1}, E_{c2}	elastic components of computer model	[N mm^{-1}]
E_D	dissipated energy	[N mm]
E_{DR}	dissipated energy ratio	[-]
E_{DRmax}	maximum value of dissipated energy ratio	[-]
E_R	elastic deformation energy	[mJ]
F	compressive load	[N]
F_m	compressive load function	[N]
F_{max}	peak value of compressive load function	[N]
s_{TTF}	standard deviation of time to failure	[s]
t	idő	[s]
t_{wM}	time between the loading and unloading cycle	[s]
w	deformation	[mm]
w_m	deformation function	[mm]
w_M	elastic deformation	[mm]
w_{max}	peak value of deformation function	[mm]
w_R	elastic deformation	[mm]
η_{sz1}	viscous component of computer model	[Ns mm^{-1}]
ω	angular velocity	[s^{-1}]
TTF	time to failure	[s]
TTF_i	inner failure time	[s]
TTF_G	frequency dependence of failure times in case of Golden apples	[s]
TTF_o	outer failure time	[s]
TTF_P	frequency dependence of failure times in case of Packham pears	[s]
$TTFi_G$	frequency dependence of inner failure times in case of Golden Delicious apples	[s]
$TTFo_G$	frequency dependence of outer failure times in case of Golden Delicious apples	[s]
$TTFi_P$	frequency dependence of inner failure times in case of Packham pears	[s]
$TTFo_P$	frequency dependence of outer failure times in case of Packham pears	[s]

1. INTRODUCTION, OBJECTIVES

1.1. Relevance and significance of the topic

The safety of agricultural and horticultural products is exposed to a serious risk, when different mechanical loads are affecting them during the harvesting, handling, transportation, and packaging processes. The various crops have different limit values of injury, and the external mechanical effects can cause several types of tissue damage: sometimes, the volume of bruise can be observed in the surface, but in most cases, the visual inspection is unable to spot the damaged tissue, therefore, the separation of these crops cannot be solved. In this case, the whole pile of fruits is endangered, because the mechanical effects are often leading to a failure in the cell structure and consequential spoiling, and this biological process is affecting the other fruits.

Although, the efficiency of automatized machine separation by shape and quality is constantly growing, the loss of handling is still an important problem: as the international studies reported, 30-40% of the products are never get to the consumer, due to the extensive amount of bruise that occurs during the fruit processing. Since the visible injuries have a negative impact to the market value of fruits and vegetables, the separation studies are aims to deliver only the impeccable quality products to the market, and these research are mostly focusing to the image processing methods: the fruits examined with hyperspectral and thermal imaging can be separated by the quality requirements and consumer demand.

Beyond the recognition of visible changes and the damage inside the fruit texture, the determination of mechanical properties also carries great importance in this area, keeping the minimization of losses an essential priority. Some stiffness parameters can be measured with non-destructive methods, applying acoustic examinations or vibration analysis. Nevertheless, to understand the causes of irreversible damage, and to determine the limit values of mechanical loads, destructive measurements must be implemented, since the failure mechanism and the mechanical resistance of the various crops can be investigated only this way.

The destructive fruit and vegetable research are based on the evaluation of the force-deformation characteristics, and these measurement results can be approximated with the results of different mathematical models developed for typical agricultural materials. The material models usually applied for other computer simulations as well, where they have an important contribution of machinery and tool development used in the fruit handling and processing field.

1.2. Objectives

In this research, a regression model of failure mechanism is developed for pome fruits, and two representative species compared during the evaluation of results. In the apple production of the European Union, the Golden Delicious apples have the largest role, and it is also an important segment in the Hungarian production as well. In addition to the apples, Packham pears are chosen for the examinations and the comparison, because of the long storability and excellent availability.

For the failure measurements, the DyMaTest material analyser was applied, which was provided by the Institute of Agricultural Engineering, Gödöllő. The instrument is developed for the compressive testing of agricultural and horticultural products. This study is focusing on the fatigue phenomenon caused by a cyclic compressive load on the fruits' surface: for the fruits, repeated mechanical effects are one of the most important risk factors during the transportation, since the irreversible damage can be reached sooner, than in the case of a static mechanical load.

After the overview of the applied methods and approaches in the literature, the most important factors and parameters of the failure characteristics must be collected and determined with appropriate accuracy during compressive measurements. For the new results, the following failure-related factors are considered during the cyclic measurements of Golden Delicious apples and Packham pears:

- using a viscoelastic model to describe the behaviour of the fruit materials,
- determining the dissipated energy indicators in relation to the failure process,
- define the time to failure (TTF) parameter and develop an appropriate measurement method to collect the time index of each rupture point.

The focus is to define the influence of the mentioned factors to the TTF parameter of the examined fruit materials. During the statistical evaluation of the resulted data, the goal is to describe the failure of time with a multiple linear regression model. The summarized objectives of the work:

- determination of the inner and outer TTF values of Golden Delicious apples and Packham pears, comparison of the frequency dependence,
- measurement of the determined viscoelastic and dissipated energy variables related to the failure mechanism, development of linear regression models, and describing the mechanical resistance in the case of the two examined fruit species.

2. MATERIAL AND METHOD

This chapter presents the working principle of the measurement device and system, the methods, and equations for the processing of the resulted data, and the mathematical model, that describes the material behaviour of the examined fruit textures.

2.1. Measurement device

The DyMaTest instrument and the measuring circuit

During the compression measurements, the surface of the fruits is loaded with a measuring pin, and for the fatigue examinations, a repeated load was adjusted. The measurements were run until the tested fruits' mechanical failure. The structure of the DyMaTest material analyser, and an examined fruit sample is shown in Fig. 1.

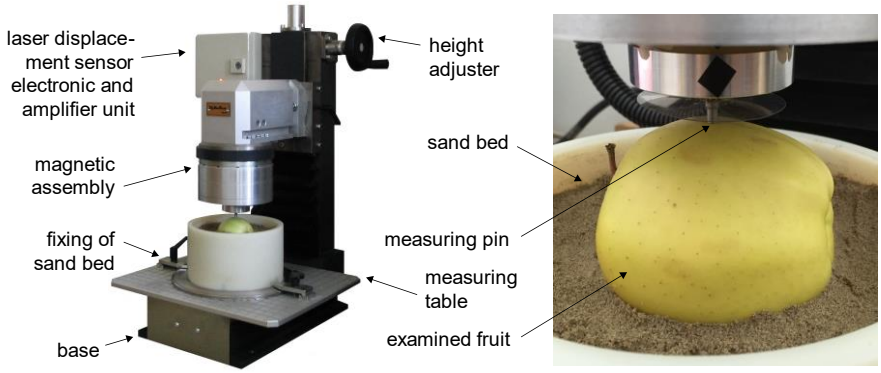

Fig. 1. Structure of the DyMaTest instrument

The deformation data can be registered by the displacement of the measuring pin, which was implemented with an OMRON ZX LT010 laser sensor in a 10 mm range, and with 3 μm resolution. This make the device capable to function in the small elastic deformation range of horticultural crops. For the force registering, a uniquely designed load cell is developed for the instrument, based on Kyowa KFG-2-120-C1-23 type strain gauges. The force and deformation data can be displayed in the function of time, the data collection was applied with 2 kHz sample rate.

The uniquely developed DyMaTest device can produce static, dynamic and repeated compressive loads: in the measurement software, linear compressive loads can be adjusted with constant and variable speed, and for the repeated examinations, sine waves of custom frequency and amplitude can be applied in the range of 0-200 Hz.

The sample is positioned in a sand bed, while the loading pin is responsible for applying the given load forces to the fruit surface (shown in Fig. 1). Before the investigations, the creeping response of the prepared sand is tested with control measurements. To perform this inspection, a solid ball bearing of 32 mm diameter is loaded. The deformation graph is not showing any creeping behaviour in the measuring range of the photoelectric sensor; therefore, the behaviour of sand is not influencing the deformation graph of the examined apple and pear fruits. The sand is dried and filtered with a mesh layer-by-layer, then it is compacted with a metal tamper.

Fig. 2 is showing the measuring circuit of the DyMaTest device. The software-adjusted compressive load signal is produced with a PC D/A card (U_{REF}) and, after the amplifying process, the analog electric signal is transformed into a dynamic effect by the electro-mechanical transducer.

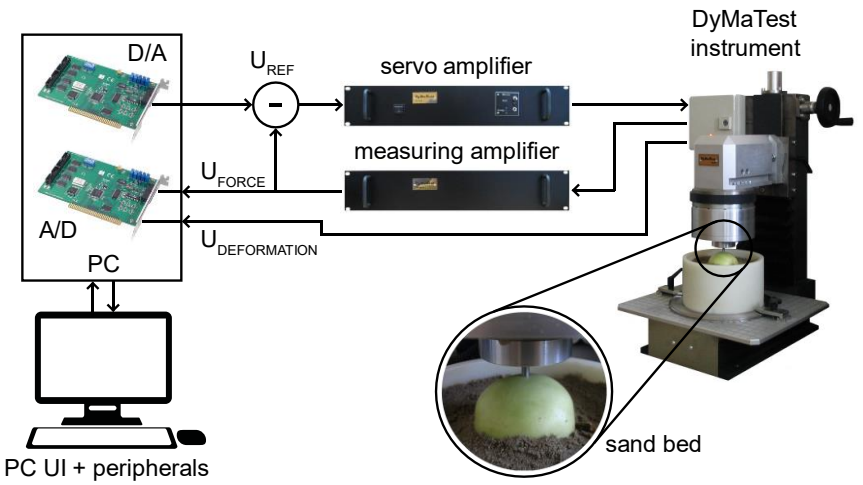

Fig. 2. Measuring circuit of the DyMaTest device

Load setups

For the current examinations, a reproducible, simple periodic force function is needed, which originates from zero, therefore, the following cosinusoidal force-function was adjusted in the software environment of the computer-controlled instrument:

$$F_m = F_{max}(1 - \cos(\omega t)), \quad (1)$$

where F_m is the measured cosinusoidal load function, F_{max} is the amplitude of the force (N), and ω is the angular velocity of the loading (s^{-1}).

Due to the different mechanical resistances of apples and pears, different magnitudes of load had to be applied. The differences originated from tissue parameters, ripeness, and storage conditions. For the Golden Delicious apples, forces under 14 N did not result in failure, but in the case of Packham pears this magnitude caused immediate disruption of the skin. Therefore, apple tests were performed with 14 N, but the pear test was completed with a 4 N magnitude of compressive load. In practice, the pears were suffered immediate rupture, when forces applied above 4 N in any frequency value of the examined range, the apples at the same time needed longer measurement time to achieve the required failure time index. Table 1 shows the load conditions implemented during the cyclic compressive tests on Golden Delicious apples and Packham pears.

Table 1. Load setups of compressive measurements

Golden Delicious			**Packham**		
Load type	**Symbol**	**Value**	**Load type**	**Symbol**	**Value**
Preload	F_{pre}	0,2 N	Preload	F_{pre}	0,2 N
Load	F	13,8 N	Load	F	3,8 N
Amplitude of load function	F_{max}	14 N	Amplitude of load function	F_{max}	4 N
Frequency	f	2,5; 3,7; 5; 7,5; 10; 11,6 Hz	Frequency	f	2,5; 3,7; 5; 7,5; 10; 11,6 Hz

According to the literature, the most dangerous frequency values were reported under 10 Hz during the transportation process, so the frequency values were adjusted in this range: the steps were divided for nearly identical intervals (2.5, 3.7, 5, 7.5, 10, and 11.6 Hz, respectively) set by practical options on the measuring device. The measurements were performed on 25 Golden Delicious specimens. Each fruit was loaded in 6 different spots, using different frequency settings, so the described viscoelastic parameters and dissipated energy values were evaluated in 300 cases overall.

2.2. Deformation graphs of Golden and Packham fruits

Fig. 3 is showing the deformation response to the cosinusoidal force function. As a result of the repeated compressive examinations, the tested biomaterial is showing a dynamic creeping behaviour: while the mean value of the cosinusoidal load is constant, the curves - that envelope the maximum and minimum points of the deformation – have a similar character to the creeping during a constant load. Since the measuring pin is not starting from the end position during the measurements, the deformation curves are not originating from zero mm at the graphs.

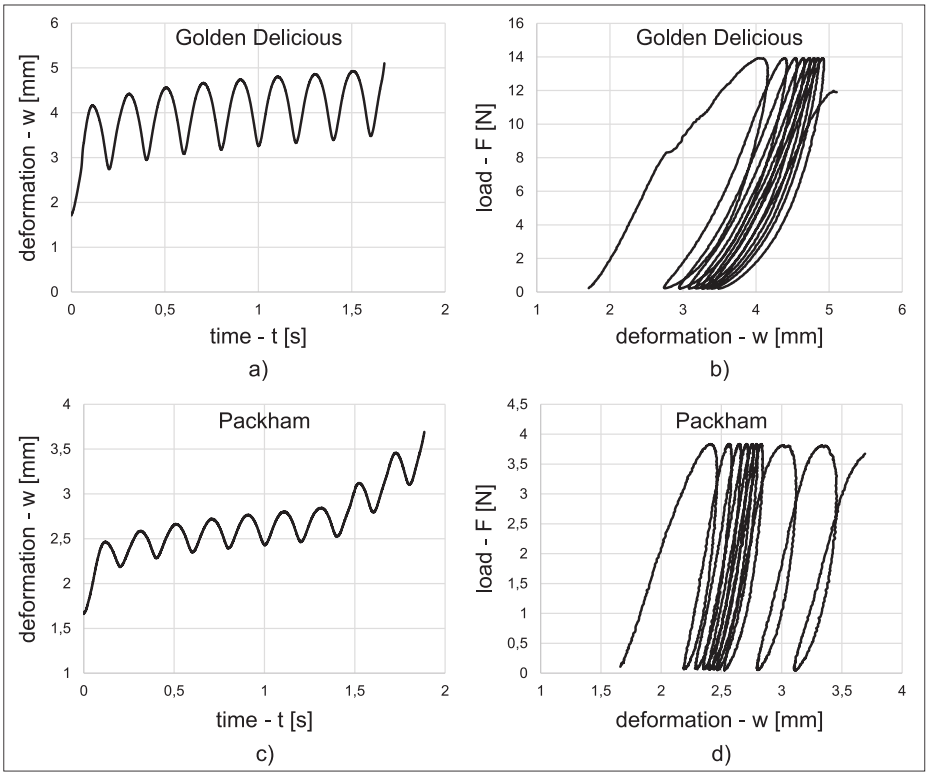

Fig. 3. Typical deformation graphs of Golden Delicious apples and Packham pears

The force-deformation curves are showing a repeated hysteresis loop (Fig 3/b and d), where the growing of permanent deformation is representing the dynamic creeping behaviour. The areas between the loading and unloading curves are in strong connection with each cycles' energy indicators.

The resulted deformation curves are investigated before the rupture point, where the irreversible failure of the fruit texture is certainly occurring. This point is determined with an image processing method, which will be explained in the next chapter.

2.3. Determination of time to failure at rupture point

For the determination of viscoelastic coefficients and energy indicators, the output data was processed until the rupture point of the fruit tissue, when the measuring pin is getting through the peel, and results a clearly visible destruction on the examined apple or pear. In this case, both peel and flesh are damaged, therefore, the material behaviour is not modelled as a homogeneous fabric, but a structure, which is built of more components.

After the rupture point, in absence of the mechanical resistance, the measuring pin is getting through the injured texture extremely fast. In the resulted graphs, the deformation curve is rising steeply after this failure moment (Fig. 4). Before the rupture point, a biological yield is also occurring, which is an initial fracture inside the microstructure of the cell system. There is no visible effect in the deformation curves for this microdamage on the inside of the fruits.

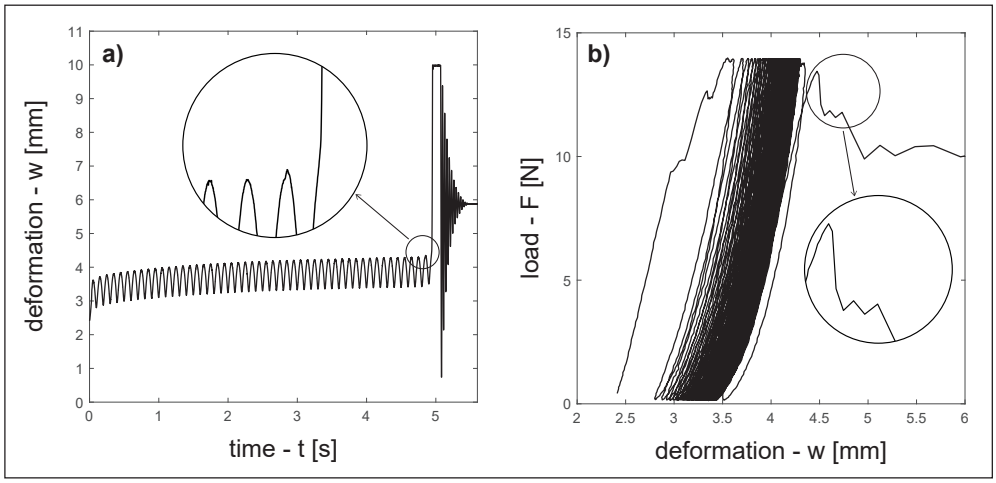

Fig. 4. Approximate area of rupture point in in case of a Golden Delicious specimen

The rupture point is somewhere between the last loading cycle and the rising curve, but similarly to the biological yield, the break point is not always showing itself.

For the precise determination of the specific occasion, the failure point is examined with a camera, which is capable of a recording with 240 frames per second. The evaluation was managed with a video editor software, where the footage can be processed by the examination of each frames. At the moment of the rupture, the measuring pin is getting through the peel, and the first frame of this fast change in the video is registered as the failure point (Fig. 5), which can be used as a time index in the subsequent data processing.

a) b)

Fig. 5. Analysis of ultra slow-motion footage

The first frame of the measuring pin movement can be synchronized to the data series, which is registered with the DyMaTest instrument, so the number of frames is transformed to the time scale of the measured results.

This time constant is defined as the examined fruit's *failure time*, or *time to failure* parameter in the present study, which is abbreviated with TTF for the subsequent data processing operations and calculations during the fatigue analysis.

Since the resolution of the camera is 4,16 milliseconds, this means the absolute error of the frame analysis. The data acquiring resolution of the DyMaTest is 8,3 times larger than the applied camera, so the failure time (which is registered from the video footage) can be placed in 8 values in the original data series. This range is highlighted in Fig. 6, which is showing an evaluated time to failure occasion.

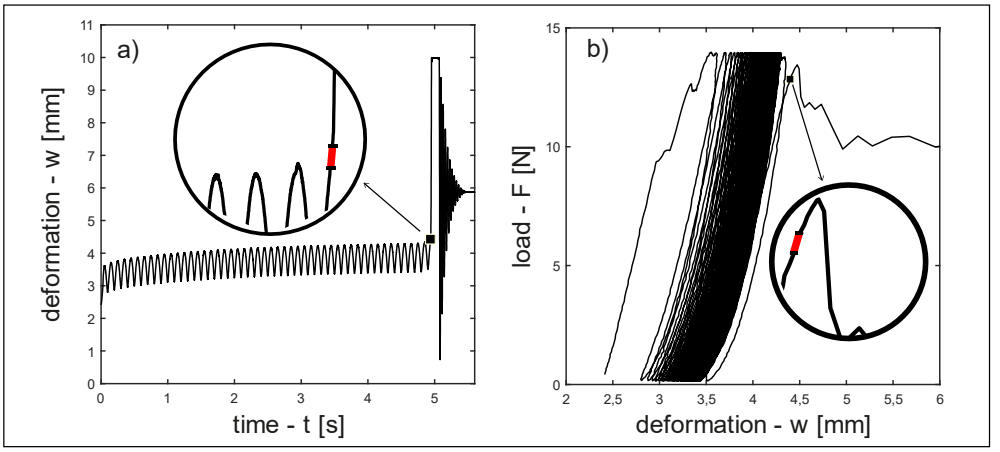

Fig. 6. Error bar of failure time calculation

2.4. Modelling of material behaviour

Viscoelastic model

Based on earlier studies, this research applies the Poynting-Thomson viscoelastic model to describe the material behaviour of the examined crops. The Poynting-Thomson body is a three-element model (Fig. 7), which is capable to characterize the stress and relaxation process of pome fruits.

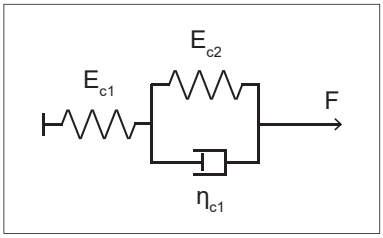

Fig. 7. The Poynting-Thomson body

The aim is to find the viscoelastic coefficients of the Poynting-Thomson equation with the best fit to the measured creep data. Compared to the previous mechanical studies, the input of the mathematical model is the measured load data instead of stress, and the output is registered as a deformation in millimetre unit instead of strain. The model presented in Fig. 7 can be described with the following equation:

$$F_m + \frac{\eta_{c1}}{E_{c1}+E_{c2}}\dot{F}_m = \frac{E_{c1}E_{c2}}{E_{c1}+E_{c2}}w_m + \frac{E_{c1}\eta_{c1}}{E_{c1}+E_{c2}}\dot{w}_m, \quad (2)$$

where E_{c1} and E_{c2} are the elastic components [N mm^{-1}] η_{c1} is the viscous part of the model [Ns mm^{-1}], F_m is the measured load [N], w_m is the measured deformation [mm], $\dot{F_m}$ is the derivative of load [N s^{-1}], and $\dot{w_m}$ is the derivative of deformation [mm s^{-1}].

Identification of computer model

The mathematical model was created in Matlab Simulink environment, and it was identified with the measured creep results, which was registered with the load cell and the laser displacement sensor. The simplified block-diagram of the system can be seen in Fig. 8, where the measured $w_m(t)$ data is compared to the calculated w(t) data. For the determination of viscoelastic coefficients, the difference between the two deformation curves must be minimized.

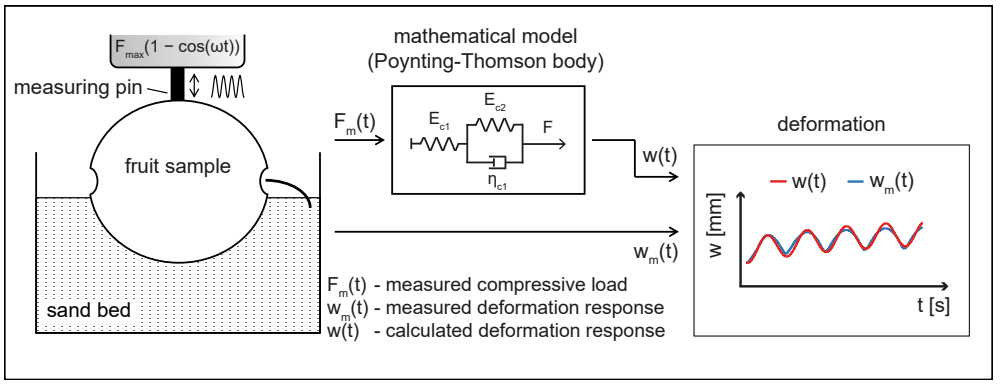

Fig. 8. Identification of computer model

The minimization process provides the best approximation for the mathematical model to the measured data:

$$w_m(t) - w(t) \rightarrow \min. \tag{3}$$

For the minimization, the least square method was applied, which can be described with the following equation for a load setup with T period:

$$\int_0^T (w_m(t) - w(t))^2 dt \rightarrow \min. \tag{4}$$

Fig. 9 is showing the block diagram of identification and minimization. The three viscoelastic properties of the 300 measurement setups can be determined within the range of 0.967–0.998 for the coefficient of determination in relation to the compared deformation outputs.

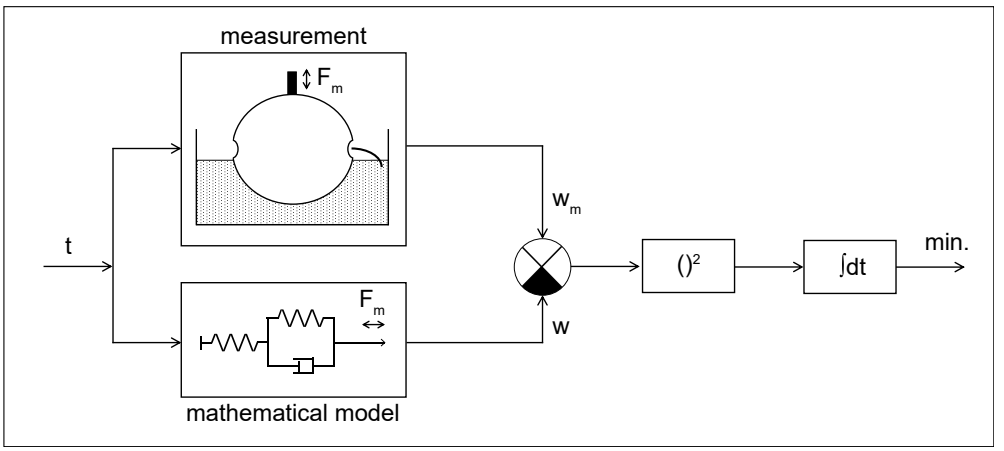

Fig. 9. System identification and minimum search

2.5. Energy calculations

Mechanical hysteresis of pome fruits

The load-deformation curve of a single load cycle from the repeated hysteresis loop is showing the energy indicators of elastic and irreversible processes (Fig. 10/a). Until the next cycle, a permanent deformation (w_M) can be seen at the bottom of the graphs. The section between the top of the curve and the end point of the unloading is representing the elastic deformation (w_R).

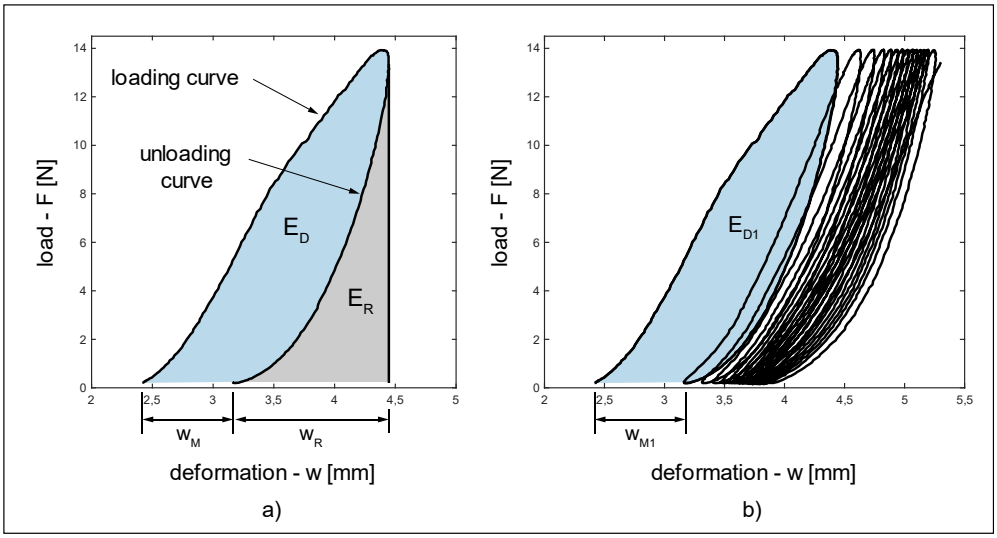

Fig. 10. Load-deformation curve in a single load cycle, and repeated hysteresis until the failure time in case of a Golden Delicious specimen

The dissipated energy can be determined with the calculation of the area between the loading and unloading curve:

$$E_D = \int_0^{t_{wM}} F \frac{dw}{dt} dt, \tag{5}$$

where E_D denotes the dissipated energy [mJ], while t_{wM} is the period of the given load cycle [s] and F is the load function [N].

Based on this equation and the measured load and deformation data, the dissipated energy can be calculated with the numeric integration of the parametric curve in case of each cycle. The Simulink based block diagram solution for the energy calculation is presented in Fig. 11, where the resulted load and deformation data from the cyclic compressive test are available as lookup-table inputs.

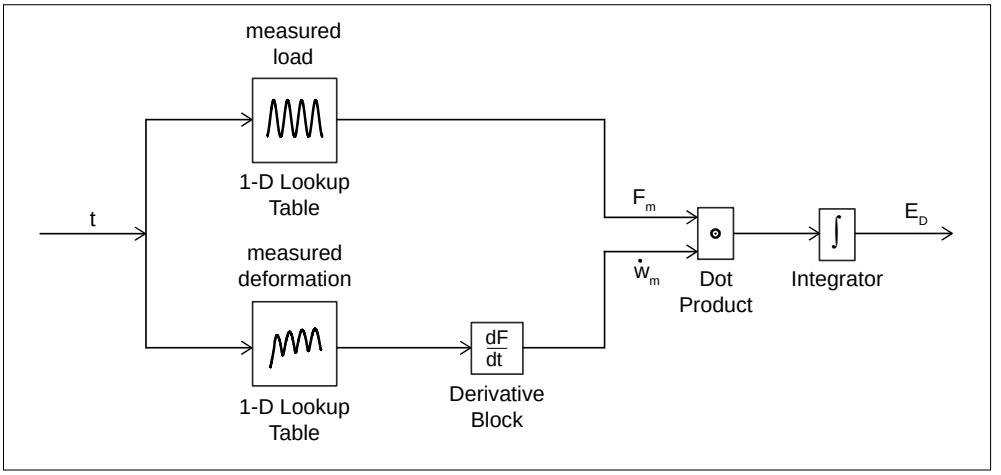

Fig. 11. Calculation of dissipated energy in Simulink environment

Determination of inner failure point

With the resulted dissipated energy values, another failure indicator can be defined. For this objective, the ratio of dissipated energy is calculated, which was previously used for the investigation of cracking propagation and failure analysis of different asphalt pavements in various studies. This ratio is described with the following formula:

$$E_{DR}=\frac{\sum_{i=0}^{n} E_{Di}}{E_{Dn}}, \tag{6}$$

where E_{Di} denotes the sum of dissipated energy at the given load cycle [mJ], and E_{Dn} is the dissipated energy of the last calculated cycle [mJ]. If this ratio is displayed in the function of load cycles (Fig. 12), a clearly visible peak value can be identified. Therefore, the fatigue failure is defined with an inner fracture from the energy calculation, and a rupture point from chapter 2.3.

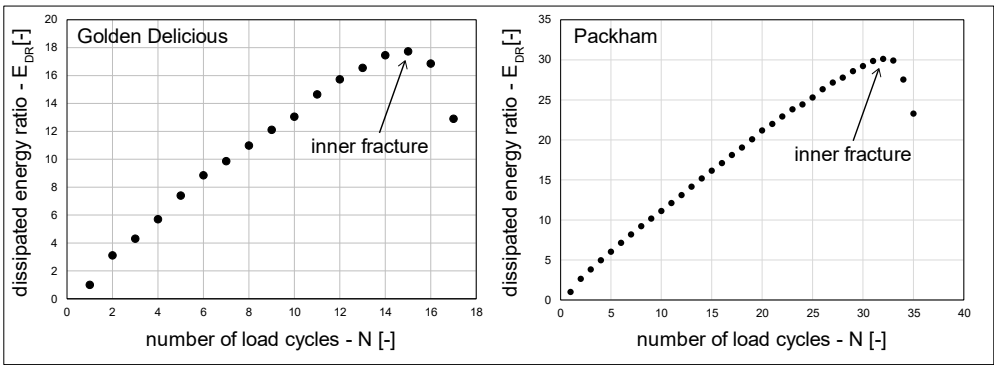

Fig. 12. Energy peak related to inner fracture during the fatigue process of Golden Delicious apples and Packham pears

2.6. Summary of the measured parameters

The measurement results, which was presented in the previous chapters are the basis of the failure regression model. Table 2 is showing the parameters.

Table 2. Resulted parameters during compressive measurements

Parameter	**Symbol**	**Description**	**Unit**
Time to failure	TTF_i	failure time until the inner rupture	s
	TTF_o	failure time until the outer rupture	s
Coefficients of viscoelastic model	E_{c1}	elastic component	N mm^{-1}
	E_{c2}	elastic component	N mm^{-1}
	η_{c1}	viscous component	Ns mm^{-1}
Dissipated energy	E_{DRmax}	maximum value of dissipated energy ratio	-
Frequency	f	frequency of the repeated load	Hz

Each fruit was loaded with six different frequency settings, (2,5, 3,7, 5, 7,5, 10 és 11,6 Hz), the measurements were performed on 25 Golden Delicious and 25 Packham specimens.

Hypothesis H1: The measured outer failure time from the frame analysis and the resulted inner failure time from the dissipated energy calculations are probably connected, and with this correlation, the rupture time inside the cell structure can be determined without the dissipated energy calculations, if the outer failure time is already known.

Hypothesis H2: With the resulted parameters from the measurements, a multivariate linear regression model can be applied for the examined pome fruits, which can be described with the

$$TTF = a + bE_{c1} + cE_{c2} + d\eta_{c1} + hE_{DRmax} \quad (7)$$

equation, where *a*, *b*, *c*, *d*, and *h* are the coefficients of the approximation.

3. RESULTS

This chapter presents the frequency dependence of the resulted time to failure parameters, the viscoeleastic coefficients and the maximum values of dissipated energy ratios from the repeated compressive measurements. The chapter also showing the applied multivariate linear regression models for the examined Golden Delicious and Packham specimens.

3.1. Evaluation of outer and inner failure times

Frequency dependence of outer failure times

According to the frequency dependence of the outer rupture points, the apples are showing less mechanical resistance in higher frequency values, therefore, the failure time occurs sooner. However, the examined pears are showing more elastic behaviour above 5 Hz, so the failure time is changing in a growing tendency in case of Packham specimens. Table 3 is showing the average values of 25 measurements in the investigated frequency range. The resulted frequency graphs, and the standard deviation can be seen in Fig. 13.

Table 3. Average values of outer failure times with satndard deviation

frequency [Hz]	**Golden**		**Packham**	
	TTF_o [s]	**standard deviation – s_{TTF} [s]**	**TTF_o [s]**	**standard deviation – s_{TTF} [s]**
2,5	6,002	3,006	1,522	1,105
3,7	3,758	1,857	1,237	0,858
5	2,505	1,383	1,203	0,847
7,5	1,639	0,762	1,451	1,114
10	1,192	0,672	2,046	1,662
11,6	0,938	0,938	3,384	2,790

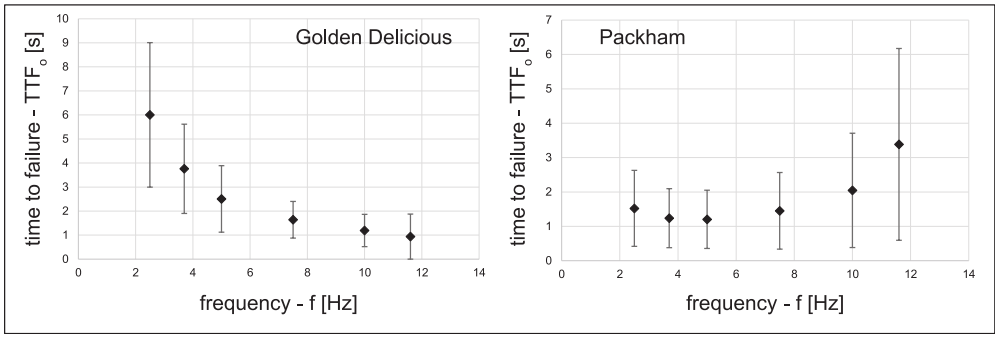

Fig. 13. Frequency dependence of outer failure times in case of Golden Delicious apples and Packham pears

According to the expectations, the failure times are registered sooner at higher frequencies in case of Golden Delicious apples, but the Packham pears showing more significant mechanical resistance in the higher section of the applied frequency range. The possible reason for this behaviour is the elastic properties of the fruit texture, which causing different fatigue characteristics for the two pome fruits. The elastic behaviour of Packham pears often provides more time before the rupture if the repeated compressive effect is happening more frequently.

Frequency dependence of inner failure times

For the comparison of inner and outer failure times, the time index of the inner rupture must be determined: at the cycle, where the maximum value of the dissipated energy ratio was registered, the inner failure must be developing during the rising of load cycle, somewhere between the starting and the end point of the compressive load ($TTF_{i\,min}$ and $TTF_{i\,max}$). The inner failure time is assigned at the average between the two extreme values (Fig. 14).

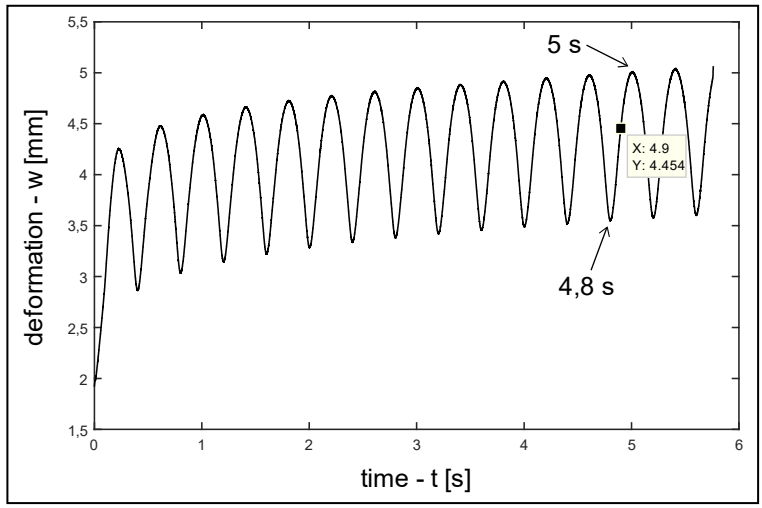

Fig. 14. Determination of inner failure time at the cycle, where the maximum of dissipated energy ratio registered

The absolute errors of evaluation at different frequency setups are presented at table 4.

Table 4 Absolute error during the evaluation of inner failure points

frequency [Hz]	2,5	3,7	5	7,5	10	11,6
absolute error [s]	0,1	0,067	0,05	$0{,}03\dot{3}$	0,025	0,022

The average values of outer failure times are presented in table 5. Fig. 15 is showing the frequency dependence of the rupture points.

Table 5. Average values of inner failure times with standard deviation

frequency [Hz]	Golden		Packham	
	TTF_i [s]	**standard deviation – s_{TTF} [s]**	**TTF_i [s]**	**standard deviation – s_{TTF} [s]**
2,5	4,804	2,727	1,081	1,015
3,7	2,997	1,783	0,771	0,673
5	1,818	1,216	0,822	0,718
7,5	1,271	0,731	1,068	0,971
10	0,905	0,619	1,927	1,586
11,6	0,703	0,596	2,958	2,644

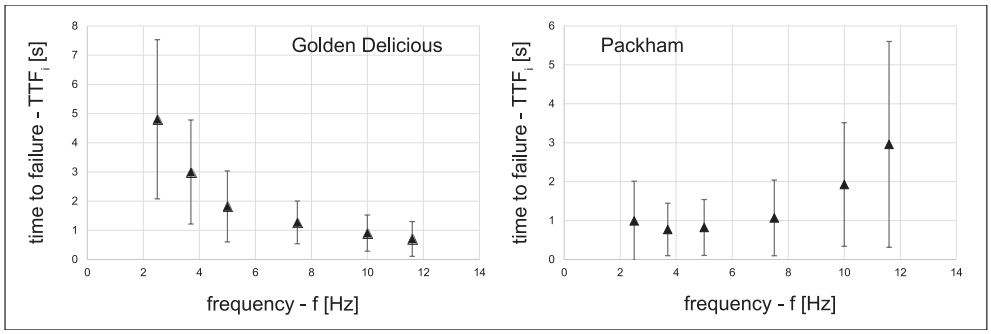

Fig. 15. Frequency dependence of inner failure times in case of Golden Delicious apples and Packham pears

According to the calculation from the energy indicators, the inner failure time values are showing the same tendency, as the results determined from the frame analysis.

Comparison of failure time parameters

At first, the ratio of inner and outer failure times were examined, but it was only correlated to the applied frequency in case of the Packham pears (the ratio is showing an increasing tendency as the frequency values growing).

Since the ratio of failure times did not show any tendency in the function of frequency in case of Golden Delicious specimens, the approximations of the frequency dependence in case of inner and outer failure times was compared. For the different tendencies, different regressions were applied, the frequency dependence of the Golden apples was described with the

$$TTF_G = a_G \, f^{-b_G} \qquad (8)$$

equation, where a_G and b_G are the coefficients of the approximation. The regression curves can be seen at the left side of Fig. 16. The graphs are also showing the equations, the accuracy of the models after the substitution is presented in table 6.

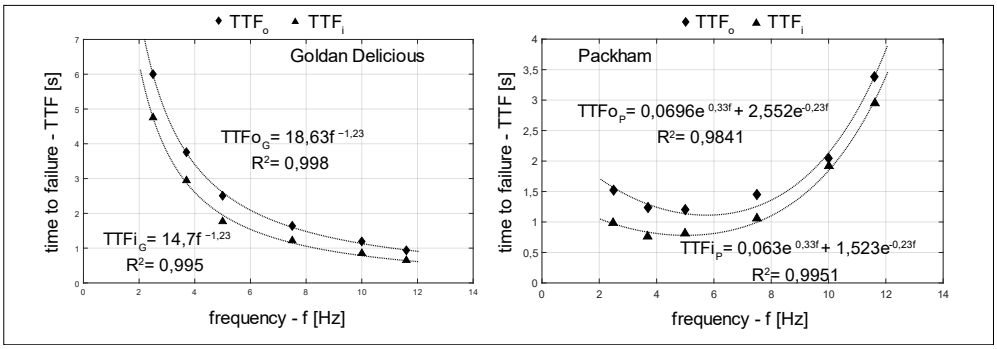

Fig. 16. Frequency dependence models of inner and outer failure times in case of Golden Delicious apples and Packham Pears

Table 6. Error of frequency dependence models in case of Golden apples

frequency [Hz]	**Golden**					
	TTF_o [s]	**$TTFo_G$ [s]**	**error [%]**	**TTF_i [s]**	**$TTFi_G$ [s]**	**error [%]**
2,5	6,002	6,036	0,553	4,804	4,763	0,879
3,7	3,758	3,727	0,849	2,997	2,941	1,907
5	2,505	2,573	2,698	1,818	2,030	11,676
7,5	1,639	1,563	4,657	1,271	1,233	2,986
10	1,192	1,097	7,981	0,905	0,866	4,362
11,6	0,938	0,914	2,562	0,703	0,721	2,555

The failure tendencies of Packham pears are quite different, so the approximation, which was used for the Golden apples must be modified. The break point at 5 Hz must be considered in the regression, so the

$$TTF_P = a_p\, e^{b_P f} + c_P\, e^{d_P f} \qquad (9)$$

equation was applied, where a_P, b_P, c_P and d_P the coefficients of the exponential process. The curves are presented at the right side of Fig. 16, the error values of approximation are summarized at table 7.

The regression curves for inner and outer failure times have the same coefficients in the exponents, so the inner failure time can be determined with the changing of the constants, if the outer failure time is already known.

Table 7. Error of frequency dependence models in case of Packham pears

frequency [Hz]	Packham					
	TTF_o [s]	$TTFo_P$ [s]	hiba [%]	TTF_i [s]	$TTFi_P$ [s]	hiba [%]
2,5	1,522	1,563	2,692	1,081	0,982	9,170
3,7	1,237	1,291	4,353	0,771	0,843	9,287
5	1,203	1,136	5,544	0,822	0,79	3,893
7,5	1,451	1,256	13,40	1,068	1,006	5,853
10	2,046	2,133	4,293	1,927	1,859	3,544
11,6	3,384	3,384	0,003	2,958	3,013	1,871

3.2. Coefficients of the viscoelastic model

According to the results, the elastic properties of Golden Delicious apples are not showing a visible frequency dependence, the E_{c1} parameter is slightly decreasing in higher frequency setups. In case of Packham pears, the E_{c1} components have a clearly increasing tendency, which is improving the mechanical resistance above 5 Hz. Both fruits are showing constant E_{c2} component in the examined frequency range. The average values of the elastic components and the standard deviation of results are shown in table 8, the frequency dependence can be seen in Fig. 17.

Table 8. Elastic components of Golden apples and Packham pears

Golden				
f [Hz]	E_{c1} [N mm^{-1}]	standard deviation [N mm^{-1}]	E_{c2} [N mm^{-1}]	standard deviation [N mm^{-1}]
2,5	10,504	1,250	2,139	0,277
3,7	10,523	1,091	2,158	0,277
5	10,546	1,497	2,116	0,292
7,5	10,622	1,529	2,139	0,269
10	10,271	1,177	2,167	0,206
11,6	9,848	1,310	1,984	0,361
Packham				
f [Hz]	E_{c1} [N mm^{-1}]	standard deviation [N mm^{-1}]	E_{c2} [N mm^{-1}]	standard deviation [N mm^{-1}]
2,5	6,896	1,710	0,554	0,160
3,7	7,705	2,184	0,518	0,177
5	7,695	2,243	0,565	0,135
7,5	8,981	1,873	0,600	0,192
10	9,730	2,540	0,613	0,130
11,6	10,178	2,172	0,623	0,127

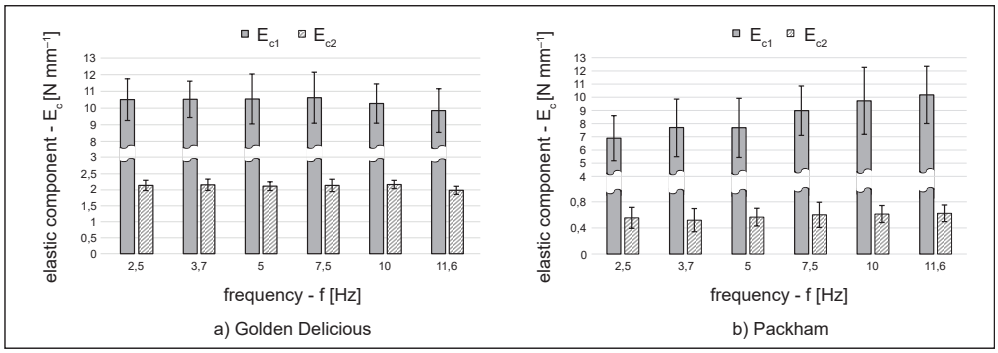

Fig. 17. Frequency dependence of elastic components

The viscous parameters of the Poynting-Thomson model are showing a frequency dependent behaviour in case of both fruit specimens, but the tendency of the Packham-related parameters is having a growing tendency at the measurement setups above 7,5 Hz. This phenomenon probably connected to the previously evaluated frequency dependence of failure time values. The average values and the standard deviation of viscous parameters can be seen in table 9, the frequency dependence is presented in Fig. 18.

Table 9. Viscous components of Golden apples and Packham pears

f [Hz]	Golden		Packham	
	η_{c1} [Ns mm^{-1}]	standard deviation [Ns mm^{-1}]	η_{c1} [Ns mm^{-1}]	standard deviation [Ns mm^{-1}]
2,5	2,129	0,703	0,848	0,494
3,7	1,429	0,358	0,574	0,226
5	1,109	0,251	0,479	0,242
7,5	0,722	0,204	0,435	0,223
10	0,581	0,154	0,436	0,243
11,6	0,509	0,106	0,471	0,239

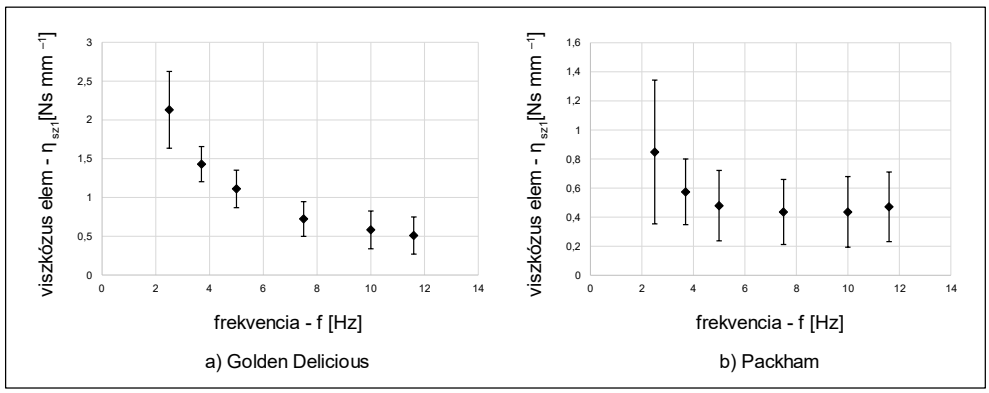

Fig. 18. Frequency dependence of viscous components

Before the failure regression modelling, the analysis of variance (ANOVA) method was used for the verification of the presented frequency dependence of viscoelastic parameters. Table 10 is presenting the results of the verification.

Table 10. Analysis of variance in case of viscoelastic properties

Golden			Packham		
coefficient	**F**	**p**	**coefficient**	**F**	**p**
E_{c1}	1,196	0,314	E_{c1}	8,008	<0,001
E_{c2}	1,408	0,225	E_{c2}	1,488	0,198
η_{c1}	75,393	<0,001	η_{c1}	6,427	<0,001

ANOVA results showed significant correlation between the η_{c1} component and the frequency in case of Golden Delicious apples. Fig. 17 does not indicate any visible tendency for elastic components, and the ANOVA results also confirmed that observation. The elastic behaviour of Packham pears has an important role in the failure characteristics, so the expected significant correlation between the E_c components and the frequency setups was also confirmed in case of E_{c1} parameters.

3.3. Linear regression models of failure behaviour

From the examined variables from the measurements, there are four regression model is resulted with different coefficients of determination for Golden Delicious apples. The models are shown in table 11.

Table 11. Linear regression model summary for Golden apples

model	**R^2**	**adjusted R^2**	**std. error of the estimate**	**F change**	**sig. F change**
a	0,814	0,812	1,03413	641,502	0,000
b	0,927	0,926	0,64922	226,984	0,000
c	0,943	0,941	0,57824	39,039	0,000
d	0,945	0,943	0,56840	6,064	0,015

a predictors: η_{c1}
b predictors: η_{c1}, E_{DRmax}
c predictors: η_{c1}, E_{DRmax}, E_{c1}
d predictors: η_{c1}, E_{DRmax}, E_{c1}, E_{c2}

In model c, E_{c1} modulus is improving the fit considerably, so this elastic parameter is reasonable to include into the characterization. However, E_{c2} is also increasing the R^2 in model d, the difference between the two options is so small, that this variable just means an unnecessary to describe the elastic behavior – the E_{c1} is representing it for the given material already. Considering these standpoints, model c is chosen with the following coefficients:

$$TTF_o = 0{,}533 + 2{,}736\ \eta_{c1} + 0{,}141\ E_{DRmax} - 0{,}261\ E_{c1}. \quad (10)$$

The models for Packham pears are presented in table 12. In addition to the results of Golden apples, the loading frequency is included in certain model options, which has an important role in the characterisation of the failure mechanism.

Table 12. Linear regression model summary for Packham pears

model	R^2	adjusted R^2	std. error of the estimate	F change	sig. F change
a	0,785	0,783	0,66044	488,514	0,000
b	0,871	0,869	0,51404	88,193	0,000
c	0,896	0,893	0,46299	31,948	0,000
d	0,920	0,917	0,40765	39,273	0,000

a predictors: E_{DRmax}
b predictors: E_{DRmax}, η_{sz1}
c predictors: E_{DRmax}, η_{sz1}, f
d predictors: E_{DRmax}, η_{sz1}, f, E_{sz2}

For Packham pears, the following equation is used:

$$TTF_o = 0{,}091 + 0{,}788\ \eta_{c1} + 0{,}085 E_{DRmax} - 0{,}103\ f + 1{,}524\ E_{c2}. \quad (11)$$

The validity of the models was also verified with the analysis of variance: the significance levels are $p<0{,}05$, so the resulted models are applicable for the quantitative description of the investigated phenomena (shown in table 13).

Table 13. ANOVA summary of the linear regression models

Golden		Packham	
F	p	F	p
792,307	<0,001	375,742	<0,001

The average results of frequency setups in case of Golden samples fall into the 1,54% - 3,85% range of relative error, and the average results of each specimens are fall between the 1,01% and 31,13% relative error values. The average values of frequency setups in case of Packham pears were resulted between 2,42 and 6,22% relative error, and the average results of each specimens are fall between the 0,04% - 34,51% range of relative error. The more significant error values are rather connecting to different mechanical resistance of the samples, and not to the applied frequency setups.

4. NEW SCIENTIFIC RESULTS

In this study, the mechanical resistance of Golden Delicious apples and Packham pears was examined with the definition and determination of failure time. The investigations focused to the fatigue failure, which was induced by six repeated compressive load setups in different frequencies. The scientific results of my research are summed up as follows:

1. *Correlation of inner and outer failure time of Golden Delicious apples*

The frequency dependence of the outer failure time ($TTFo_G$), which was determined with the frame analysis, and the inner failure time ($TTFi_G$), which was calculated from the dissipated energy ratio are described with the following, identical exponent equations:

$$TTFo_G = 18{,}63\ f^{-1{,}23},$$

$$TTFi_G = 14{,}7\ f^{-1{,}23},$$

where f is the frequency of the compressive load. Because of the different stress-deformation curves, there was no unified method for the determination of the two failure times in the previous studies. With the defined approximations, the dissipated energy calculations can be avoided, and the inner failure time can be determined, if the outer failure time is known. In the examined range (2,5-11,6 Hz), the equation for the average values of outer failure time describes the frequency dependence with 7,98% maximum error, and the approximation for the inner failure time is characterizing the frequency dependence with 11,67% peak value of error.

2. *Correlation of inner and outer failure time of Packham pears*

Like in the case of Golden specimens, the resulted outer failure time ($TTFo_P$) from the frame analysis measurements, and the calculated inner failure time ($TTFi_P$) from the energy indicators are described with the following, identical exponent equations:

$$TTFo_P = 0{,}069\ e^{0{,}33f} + 2{,}552\ e^{-0{,}238f},$$

$$TTFi_P = 0{,}063\ e^{0{,}33f} + 1{,}523\ e^{-0{,}238f},$$

where f is the frequency of the compressive load. In the examined frequency range of the study (2,5-11,6 Hz), the equation for the average values of outer failure time describes the frequency dependence with 13,4% maximum error, and the approximation for the inner failure time is characterizing the frequency dependence with 9,29% peak value of error.

3. Linear regression model for the failure time of Golden Delicious apples

With the using of the Poynting-Thomson body coefficients (the E_{c1} and η_{c1} components), and the maximum value of dissipated energy ratio (E_{DRmax}), a multiple linear regression model is created to describe the failure time of Golden Delicious apples:

$$TTF_o = 0{,}533 + 2{,}736\ \eta_{c1} + 0{,}141\ E_{DRmax} - 0{,}261\ E_{c1}.$$

In the examined range (2,5-11,6 Hz), the equation is describing the average time to failure results of frequency setups with 3,85% maximum error, and the average failure time values of specimens with 31,13% maximum error.

4. Linear regression model for the failure time of Packham pears

For the approximation of failure time, the E_{c2} elastic, and the η_{c1} viscous component was used from the Poynting-Thomson model, and besides the E_{DRmax} parameter, the applied frequency value is also influencing the failure process. Therefore, the applied equation for the failure time:

$$TTF_o = 0{,}091 + 0{,}788\ \eta_{c1} + 0{,}085\ E_{DRmax} - 0{,}103\ f + 1{,}524\ E_{c2}.$$

In the examined frequency range (2,5-11,6 Hz), the equation is describing the average time to failure results of frequency setups with 6,22% maximum error, and the average failure time values of specimens with 34,51% maximum error.

5. CONCLUSIONS AND SUGGESTIONS

The developed measuring methods and the resulted equations of this study were focusing to characterize the failure mechanism of Golden Delicious apples and Packham pears. The outer failure time of the examined fruits (which is defined as rupture point in the literature) was determined with the frame analysis of an ultra-slow-motion camera footage. The inner failure time was calculated from the dissipated energy ratio, which was implemented from another research area to the present investigations of fruit materials.

Knowing the failure limits inside the cell structure is essential in fruit processing, since the mechanical effects (e.g. handling, dropping or vibration) from the environment must be limited or modified by the results of research. With the inner rupture point from the energy calculations, the equations for the frequency dependences can describe the connection between the inner and outer failure times, so the determination of outer rupture is sufficient for the mapping of the inner failure process, if the number of samples is chosen appropriately for the measurements.

The failure characteristics are in strong correlation with the material properties and energy indicators, and with these parameters, the mechanical resistance can be described, using the simplest linear approximation. The relative error during the application of the linear models is composed of three different aspects in the level of compressive measurements and data processing methods:

1. The coefficients of the Poynting-Thomson model were also determined with a regression method during the parameter identification, which is also carries an uncertainty. The area between the two curves can be different in case of the fruit specimens.
2. The frame analysis for the registration of outer rupture time also carrying the possibility of error, since the sample rate has its own limitations.
3. The E_{DRmax} value is indicating the inner rupture of some level, but the accurate background of this relationship is still waiting for more investigations.

Since the handling processes begins after the fruit picking, the failure investigations must be implemented during the unripe stage of fruits as well. In this case, different limit values of mechanical effects could be dominating compared to other products, which can be purchased at the market. The models can be modified with the consideration of ripening status, described with more control parameters (e.g. moisture content). The usability of models can be compared with the results of longer compressive loading periods, which can be achieved with an improved infrastructure of informatics.

6. SUMMARY

FAILURE CHARACTERISTICS OF BIOLOGICAL MATERIALS

Since several mechanical effects risking the safety of the horticultural products after the picking, studying the damage resistance and failure susceptibility of fruits are one of the most important topics in food processing and logistics. A very significant amount of the crops never gets to the costumer, because the mechanical effects are often causing a surface injury or an extended bruise inside the fruit, leading to a failure in the cell structure and consequential spoiling of the product, decreasing market value. From the variety of different mechanical effects, the repeated compressive loads are one of the most important risk factors during the postharvest procedures of fruits, which are originated from machine vibrations.

This work focuses the fatigue failure of selected pome fruits, which is caused by repeated compressive loads. A multiple linear regression model of mechanical properties related to the failure mechanism of Golden Delicious apples and Packham pears tissue under repeated compressive load is investigated. The model predicts the mechanical resistance of the examined pome fruits.

For this study, the following failure-related factors are considered during the cyclic measurements of the examined specimens: the material behaviour, which is described with viscoelastic parameters, the dissipated energy indicators during the compressive loading process, and the outer rupture point of the cell-structure, which is described with the time to failure (TTF) parameter.

With a mathematical model, the elastic and viscous coefficients was determined during a minimum search method, which are calculated at the best fit to the measured creep data.

The accumulation of energy during the repeated compressive measurements, and the calculation of dissipated energy ratio from the hysteresis loop of the stress-strain characteristics are strongly connected to the inner rupture point of the crop, which can be set as the limit value of mechanical effects during the design of machine parts and processing environments. The relationship between the outer failure time, which is determined with frame analysis, and the inner failure time, which is calculated from the energy indicators can be described, so the inner rupture point can be determined without the energy analysis. In addition, the outer failure time of Golden Delicious apples and Packham pears can be predicted based on the measured failure-related parameters obtained during the compressive load tests.

7. MOST IMPORTANT PUBLICATIONS RELATED TO THE THESIS

Referred articles in foreign languages

1. **Farkas, C.**, Petróczki, K., Fenyvesi, L. (2016): Method for measuring fruit failure caused by different mechanical loads. Hungarian Agricultural Engineering, (29), pp. 51-54. ISSN 2415-9751
2. **Farkas, C.**, Fenyvesi, L., Petróczki, K. (2019): Identification and Frequency Dependence of Viscoelastic Parameters during Dynamic Creep Tests on Selected Pome Fruits. AgriEngineering, 1(3), pp. 324-331. ISSN 2624-7402
3. **Farkas, C.,** Fenyvesi, L, Petróczki, K. (2019): Multiple linear regression model of Golden apple's failure characteristics under repeated compressive load. Potravinarstvo Slovak Journal of Food Sciences, 13(1), pp. 793-799. ISSN 1337-0960

Referred articles in Hungarian language

4. **Farkas, C.**, Fenyvesi, L., Petróczki, K. (2019): Almásterméső gyümölcsökben kialakuló energiatranszport-elemzés ismétlődő terheléssel végzett roncsolásos vizsgálat útján. Mezőgazdasági Technika, 2019/07, pp. 2-5. ISSN 0026 1890
5. **Farkas, C.**, Fenyvesi, L., Petróczki, K. (2019): Vilmos körték viszkoelaszikus paramétereinek és energiamutatóinak terhelésfüggése ismétlődő mechanikai igénybevétel hatására. Mezőgazdasági Technika, 2019/10, pp. 2-5. ISSN 0026 1890
6. **Farkas, C.**, Fenyvesi, L., Petróczki, K. (2020): Golden Delicious almák és Vilmos körték kifáradási mutatóinak összehasonlítása. Élelmiszervizsgálati Közlemények, ISSN 2676 8704 – Accepted for publication.